Available online at www.sciencedirect.com

ScienceDirect

Energy Procedia 4 (2011) 4371–4378

Energy Procedia

www.elsevier.com/locate/procedia

GHGT-10

A Sensitivity Study on Regional Pressure Buildup from Large-Scale CO_2 Storage Projects

J.T. Birkholzer*, Q. Zhou, A. Cortis, S. Finsterle

Lawrence Berkeley National Laboratory, 1 Cyclotron Road, MS 90-116, Berkele, CA 94707, USA

Abstract

Several international researchers have in recent years evaluated the potentially far-reaching brine pressurization and migration processes resulting from the storage of large volumes of CO_2 in deep saline aquifers (e.g, [1]-[6]). Predictive simulations have been conducted for idealized geologic systems as well as for large sedimentary basins with promising CO_2 sequestration potential. In contrast to the latter studies, which often involve laterally extensive sediments with large storage capacity, we investigate here the potential impact of geologic carbon sequestration in a partially compartmentalized sandstone basin in the Southern San Joaquin Valley in California, USA. The expected CO_2 plume behavior and injection-related pressure perturbation are modeled for a hypothetical CO_2 sequestration project situated in the center of the basin. Uncertainty about fault behavior is addressed by assessing two distinctive fault property scenarios. A systematic sensitivity study is conducted for each scenario to identify key parameters and processes affecting pressure buildup and brine migration. We distinguish in this sensitivity study between the near-field region comprising the projected size of the CO_2 plume, where hydrogeological properties are expected to be better constrained, and the far-field region comprising the projected extent of pressure buildup, where parameter uncertainty can be quite high.

Keywords: brine pressurization; basins; faults; compartments;

1. Introduction

If carbon dioxide capture and storage (CCS) technologies are implemented on a large scale, the amounts of CO_2 injected and sequestered underground will be very large. Various research studies have been conducted to date evaluating under which hydrogeological conditions the injected volumes of CO_2 can be safely stored over hundreds or even thousands of years. For example, many of these studies address issues such as the long-term efficiency of structural trapping of CO_2 under sealing layers, or the importance of other trapping mechanisms such as dissolution of CO_2 into formation water or mineral trapping as CO_2 reacts with the rock. Less emphasis has been placed on the issue of regional-scale pressure buildup and brine migration in saline reservoirs, as native brines are displaced by the injected CO_2. Industrial-scale injection of CO_2 may impact subsurface volumes that can be significantly larger than the CO_2 plume itself. Thus, even if the injected CO_2 is safely trapped in suitable geological structures, injection-

* Corresponding author. Tel.: +1 510 486 7134; fax: +1 510 486 5686.
E-mail address: jtbirkholzer@lbl.gov.

doi:10.1016/j.egypro.2011.02.389

related pressurization may jeopardize caprock integrity and impact groundwater resources. As an example of the latter, overpressure over much of a basin can provide a driving force pushing brine upward into overlying freshwater aquifers via possibly existing localized pathways.

Several researchers have recently conducted predictive studies for hypothetical sequestration scenarios to evaluate the pressure and brine displacement response to future industrial-scale carbon sequestration, first for idealized geologic systems. For example, a simulation study of CO_2 injection into compartmentalized saline formations [7] suggests small storage capacity in such bounded systems because strong pressurization occurs and geomechanical damage must be avoided. Birkholzer et al. [3] reported far-reaching pressure perturbations in an idealized, laterally open groundwater system that allows displaced brine to migrate into other parts of the formation or into neighboring formations. Predictive simulations were also conducted for more complex situations based on real groundwater systems ([2], [4], [5], [6]). Common to these "real-world" applications is that they are representative of extensive "open" sedimentary basins where storage capacity is expected to be large and reservoir compartmentalization plays no role.

The current paper describes a predictive study of large-scale pressure buildup and brine migration for a hypothetical storage project in the Southern San Joaquin Basin (as defined in [8]) in California, USA, which has significant storage resources. However, its stratigraphic and structural complexity, caused by the existence of numerous faults, may provide an "end member" condition opposite to the regional groundwater systems described above. Some of these faults may be sealing, while others may be conductive. Our study evaluates the potential for reservoir compartmentalization and the corresponding impact on pressurization in such systems. Section 2 below describes the simulation model developed for the Southern San Joaquin Basin and discusses prediction results for two fault property scenarios. Considering the relevance of the pressure impacts and the importance of understanding model uncertainty, a systematic sensitivity study is conducted for both scenarios to identify key parameters and processes affecting pressure buildup and brine migration (Section 3). We distinguish in the sensitivity study between the near-field region comprising the projected size of the CO_2 plume, where hydrogeological properties are expected to be better constrained, and the far-field region comprising the projected extent of pressure buildup, where parameter uncertainty may be higher.

2. Forward Modeling of Hypothetical CO_2 Storage Project in the Southern San Joaquin Basin

2.1 Model Domain and Setup

The model domain for CO_2 storage in the Southern San Joaquin Basin covers a large region of 84 km in the eastern direction by 112 km in the northern direction. The hypothetical injection site for this study is located in the center of the basin, where the Vedder Sand offers a viable storage option. The formation dips upward towards a shallow outcrop area located along the eastern model boundary, at an average slope of 7°. The Vedder Sand is quite permeable providing for sufficient injectivity, and the overlying Temblor-Freeman Shale is considered a suitable caprock for stratigraphic containment of the injected supercritical CO_2. At the injection site, the Vedder Sand is 400 m thick, and its top elevation is -2,751 m. The caprock (the Freeman Shale) is about 200 m thick. The hypothetical storage scenario is that 5 Mt CO_2 per year will be injected for 50 years.

Two different 3D mesh discretizations have been generated for the purpose of this study, both comprising the entire stratigraphy from the ground surface to the basement granite. The discretization shown in Figure 1 is used for forward simulations, where computational efficiency is not as crucial as in the sensitivity studies. This 3D mesh has a total of 470,573 elements, arranged in 77 2D model layers. Seven major fault zones are explicitly represented. The Vedder Sand is divided into six alternating sand/shale layers honoring the observed geology at a large number of geologic logs in the model domain. The thickest sand layer (the first Vedder Sand) is located at the top portion underlying the Temblor-Freeman Shale. The second discretization, a less refined version of the one shown in Figure 1, incorporates many of the salient model features, such as explicit representation of fault zones and the sand/shale interbedding within the Vedder Sand, but overall has considerably less refinement, with a total of 21,803 elements. The purpose of this reduction in mesh refinement is to speed up the simulation runtime such that a large number of sensitivity runs can be conducted within reasonable time constraints. Results between the two meshes have been compared to ensure that the coarse discretization is adequate for the purpose of this study.

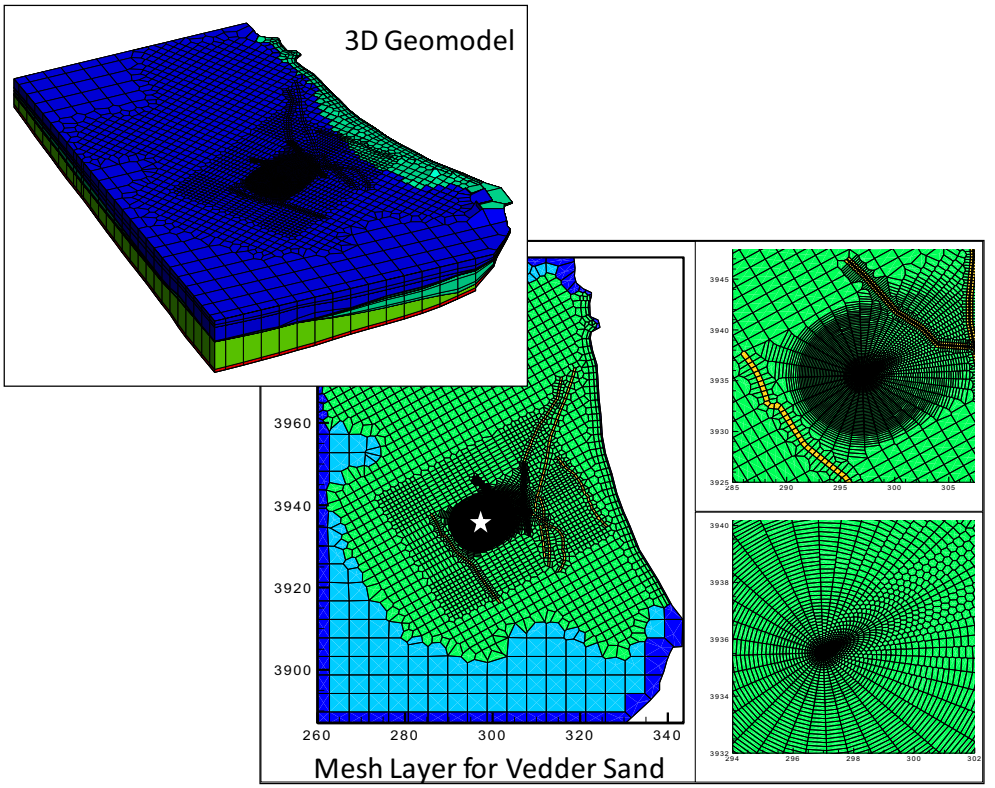

Figure 1. 3D geological model (top) and discretization in a 2D planview for one of the Vedder Sand layers (bottom). White star shows injection location. The green color represents the region with presence of the Vedder Sand. Yellow color represents faults. Boundary elements are in blue.

Table 1 shows the hydrogeologic properties assigned for each formation, based on site characterization data available from oil and gas exploration and groundwater development in the area. Fault zone properties are quite uncertain; however, there are qualitative observations that most major fault zones should be less conductive than the adjacent sandstone formations: (1) oil and gas trapping is observed under in situ effective stress conditions, (2) water-level observations in the Pond-Poso-Creek fault zone east of the hypothetical injection location suggest a partial groundwater barrier in shallow units, and (3) oil and gas fields are partially compartmentalized as evidenced by pumping tests. While acting as partial barriers, the fault offset is in all cases much smaller than the thickness of the Vedder Sand; thus some lateral hydraulic connectivity across the faults is to be expected. For the purpose of this study, where we are mostly interested in pressure perturbation and brine displacement, we consider two basic property scenarios: (a) a *fault scenario* representing partial compartmentalization where the lateral fault permeability of all major faults is reduced by a factor of 100 compared to the adjacent formation permeability, and (b) a *no-fault scenario* where all fault properties are set identical to the adjacent formation. In the former scenario, the most prominent faults that were assigned such reduction are the Greeley fault west of the injection location and the Pond-Poso-Creek fault zone east of the injection location. Many additional fault property scenarios were studied, but shall not be reported here. Note that in all scenarios, faults are assumed non-conductive in shale formations; i.e., the potential for leakage of CO_2 and/or brine through permeable faults is not a concern in this study.

Initial conditions for pressure, temperature and salinity were interpolated based on their observed correlation with depth; hydrostatic conditions were assumed for the initial flow field. Boundary conditions were selected as follows: the eastern, northern and western boundaries are of fixed pressure, salinity, and temperature, while the southern boundary is closed. Displaced water can easily escape from the system through the eastern boundary, where the

outcrop of the Vedder Sand is located. Since the Vedder formation is a freshwater resource at this outcrop, the flux of formation water towards the eastern boundary is an important model output. Much less displaced water can escape through the northern, western, and southern boundaries, because the Vedder Sand pinches out there and is thin to absent along these boundaries.

Table 1. Hydrogeologic properties assigned to each formation: k_h is horizontal permeability, k_v is vertical permeability, Φ is porosity, β_p is pore compressibility, α is the van Genuchten parameter for entry capillary pressure, and m is the van Genuchten parameter for pore-size distribution.

Formations	k_h [mDarcy]	k_v [mDarcy]	Φ [-]	β_p [10^{-10} Pa^{-1}]	α [10^{-5} Pa^{-1}]	m [-]
Non-Fault Zones						
Pre-Etchegoin	3000	3000	0.35	15.5	5.0	0.457
Etchegoin	1200	1200	0.32	15.5	5.0	0.457
Macoma-Chanac	1900	1900	0.31	10.5	5.0	0.457
Santa Margarita-McLure	2000	2000	0.275	10.5	5.0	0.457
Stevens Sand	240	48	0.22	10.5	5.0	0.457
Fruitvale-Round Mountain	0.002	0.001	0.338	14.5	0.42	0.457
Olcese Sand	170	34	0.336	4.9	5.0	0.457
Temblor-Freeman	0.002	0.001	0.338	14.5	0.42	0.457
Vedder Sand (sand layers)	303	60.6	0.264	4.9	13.0	0.457
Vedder Sand (shale layers)	0.1	0.05	0.32	14.5	0.42	0.457
Tumey-Eocence	0.07	0.07	0.07	14.5	0.42	0.457
Baserock	0.0001	0.0001	0.01	22.7	0.5	0.457

2.2 Model Results

All simulation runs were conducted using the massively parallel version of the TOUGH2/ECO2N simulator ([9]-[10]). The simulation time includes the injection period of 50 years and a post-injection period. The focus of our discussion here is on the pressure and flow field perturbations generated by injection, less so on the details of CO_2 movement and trapping. For completeness of information, we shall only mention that the CO_2 plume in the Vedder Sand migrates slowly updip in the north-eastern direction, eventually approaching the Pond-Poso-Creek fault in the early stages of the post-injection period. The plume behavior experienced at the fault depends on the modeling scenario. If reservoir compartmentalization is considered as in the *fault scenario*, CO_2 initially accumulates and spreads out sideways along the fault because of its trapping effect, but entually breaks through and continues migrating updip, albeit very slowly. The maximum CO_2 plume size is about 13 km in north-eastern direction and about 9 km in north-western direction.

Figure 2 shows the pressure increase within the Vedder Sand at 10, 50, and 100 years after start of injection. Pressure perturbation in response to injection of CO_2 is fast and widespread, due to sufficient permeability in the sands, and pressurization at the formation boundaries (black outline north, south, and west) is clearly noticeable at 50 years, the end of the injection period. As pointed out before, the eastern boundary is modeled as a fixed-pressure condition, to allow for brine escaping from the model domain at the outcrop of Vedder Sand; thus pressure increase remains zero there. Pressure reduces slowly after injection stops, due to pressure bleed-off into overlying units and water losses across the lateral boundaries. There are clear differences between the two fault property scenarios. The *fault scenario* generates overall stronger pressure response since pressure propagation and brine flow away from the injection location are constrained by the reduced cross-fault permeability. Initially, this stronger pressure response is

limited to the near-field region between the Greeley and Pond-Poso-Creek faults (e.g., at 10 years), but later becomes evident in almost the entire Vedder Sand (e.g., at 50 years). Maximum pressure values are about 30 bar in the *fault scenario* and about 23 bar in the *no-fault scenario*. The differences between the two scenarios diminish after injection stops. Both scenarios exhibit small pressure increases of up to 2 bar in the overlying Olcese Sand, an indication of pressure bleed-off through the primary seal (not shown in this paper).

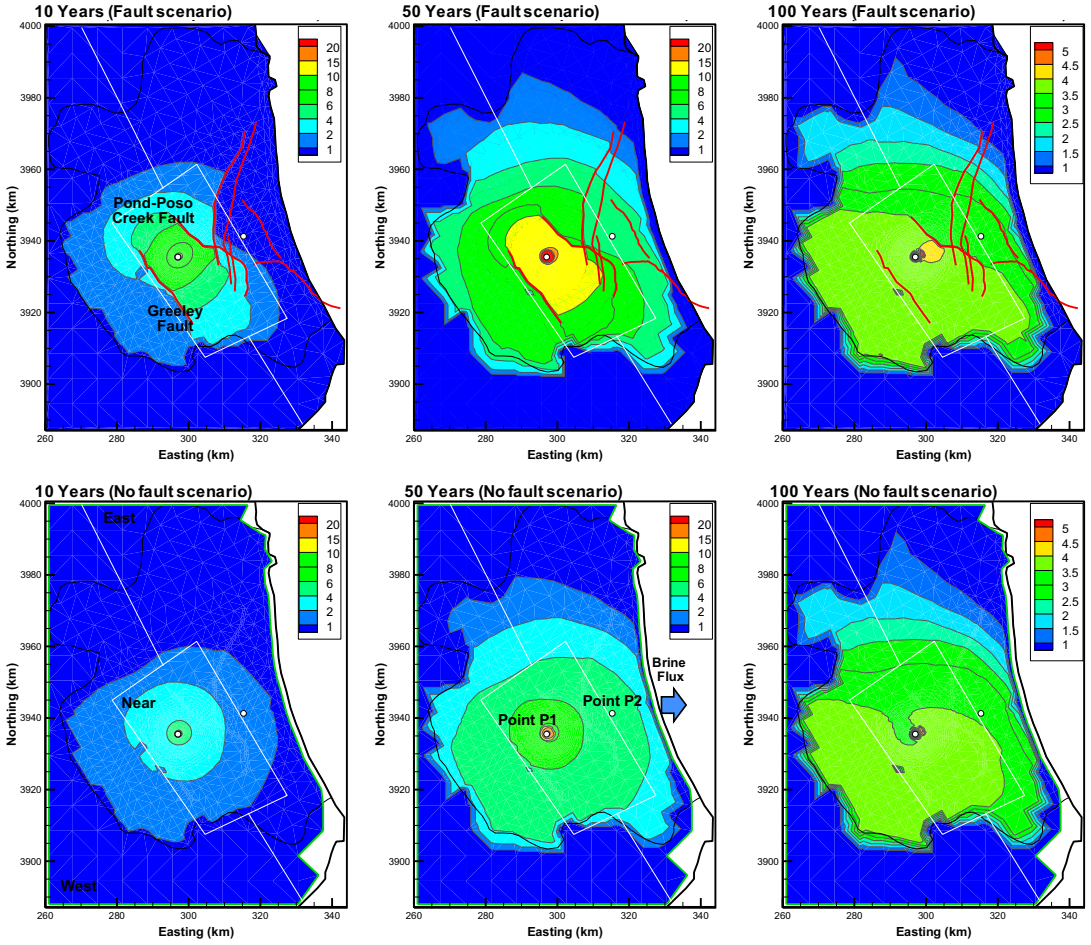

Figure 2. Pressure increase (in bar) in the Vedder Sand for both fault property scenarios, at 10, 50, and 100 years. The white lines indicate the boundaries of the near-field, eastern, and western sensitivity regions. The two small white circles in the lower middle plot are observations points P1 and P2.

3. Systematic Sensitivity Study

3.1 Sensitivity Approach

A local sensitivity analysis is performed using the iTOUGH2 simulation-optimization code [11]. The partial derivatives of representative output variables with respect to select input parameters are numerically evaluated by the perturbation method. PEST-style template and instruction files are used, respectively, to pass input parameters updated by the iTOUGH2 sensitivity analysis routines to the TOUGH2-ECO2N model, and to retrieve the calculated system state of interest from the output file [12]. To make the resulting sensitivity coefficients non-dimensional and thus comparable with each other, they are scaled by the expected input parameter uncertainty and

by the inverse of the acceptable variability in the output variables, which represent performance measures. Both input parameters and output measures may be transformed combinations of multiple model input and output variables. For example, we evaluate the sensitivity of the total brine outflow across the eastern model boundary (a combination of flow through various boundary elements) as a result of varying all permeabilities within a certain model region (a combination of several grid elements) by a constant factor. Given the nonlinear nature of the problem, the sensitivity coefficients are local, i.e., they refer to the conceptual model and reference parameter set used for the analysis. Thus, the *fault scenario* and the *no-fault scenario* need to be evaluated separately.

The dimensionless sensitivity coefficients contain basic information about the relative significance of an uncertain parameter on the relevant system behavior as represented by specific performance measures. Conversely, they can be used to evaluate which potential field observation contains information about a parameter that might be estimated by inverse modeling. Finally, the analysis can also reveal potential correlations among parameters, expected estimation uncertainties, and the uncertainties in model predictions.

3.2 Parameters Varied and Performance Measures

The input parameters varied in the sensitivity study are permeability, pore compressibility, and porosity, separately perturbed for the sand layers in the Vedder formation, the shale layers in the Vedder formation (not discussed here), as well as the overlying caprock, the Temblor-Freeman shale. We furthermore distinguish the near-field region comprising the projected size of the plume (see Figure 2), where hydrogeological properties are expected to be better characterized, and two far-field regions, the deeper western part and the updipping eastern part of the model domain. In total, with three input parameters, three formation types, and three regions, we have 27 sensitivity parameters to vary. Input parameter uncertainty is estimated as follows: a one-order-of-magnitude variation in permeability, a factor-of-five variation in pore compressibility, and a 30%-variation in porosity. Initially, these uncertainties are assumed equal in all three regions, but we later allow for different uncertainty for the near-field and the far-field regions, respectively. Output variables of interest are pressure change and brine flux. In total, we selected 10 locations to query pressure sensitivity. At each location, we evaluate pressure change in the Vedder Sand (to understand the injection reservoir response) and in the overlying Olcese Sand (to understand the pressure response above the primary seal). As an additional performance measure, we evaluate sensitivity to total brine flux across the eastern model boundary. As mentioned above, the resulting sensitivity coefficients are scaled using above listed input parameter uncertainty and an acceptable output variability of 1 bar for pressure and 1kg/s for total flux.

3.3 Selected Sensitivity Results and Discussion

We focus our discussion of sensitivity results on three performance measures: pressure observations at Point P1 in the Vedder Sand (the injection location), total brine flux across the eastern model boundary, and pressure observations at Point P2 in the Vedder Sand (a location between the updip Pond-Poso-Creek fault and the eastern model boundary) (see Figure 2). We concentrate first on sensitivity to permeability variation and start with the *fault scenario*. An exhaustive discussion of all other observed sensitivities is not possible due to space limitations; we believe that the selected results presented here provide a good idea as to what type of system understanding can be gained from a systematic local sensitivity analysis.

Figure 3(a) shows dimensionless sensitivity of pressure change at the injection location P1 in the Vedder Sand, for several discrete time steps at 5, 10, 20, 30, 45, 49, 50, 55, 60, 75, 100 years. Sensitivity is queried for six parameter variations: the Vedder Sand permeability in the three model regions and the Temblor-Freeman permeability in the three model regions. Not surprisingly, the near-field sand permeability is by far the most significant parameter for pressure perturbation at P1, followed by the Vedder Sand permeability in the western far-field region, which is closer to the injection location than the eastern far-field region. These results are obtained assuming the same permeability uncertainties in all three regions. We may instead assume that the near-field permeability uncertainty is lower by a factor of 2 (i.e., better characterized) and the far-field uncertainties are higher by a factor of 2 (i.e., less well characterized). In this case, permeability in the western far-field region is almost as significant as in the near-field region during the injection period. After injection stops, it becomes even more significant than the near-field permeability. This suggests that site characterization in far-field regions can be important in reducing prediction uncertainty for pressure buildup near the injection location (Figure 3(b)).

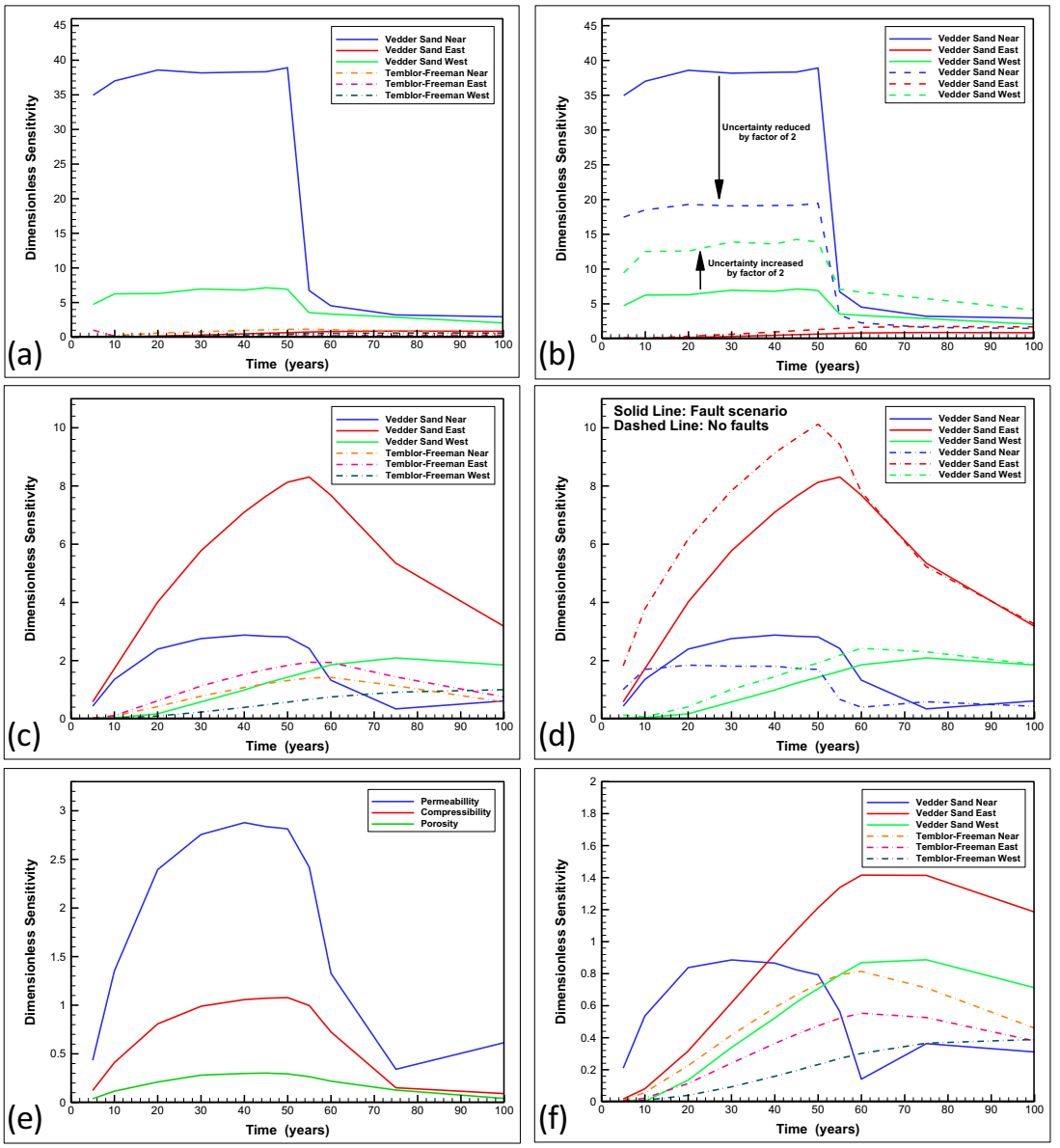

Figure 3. Dimensionless sensitivity to pressure buildup vs. time, for fault scenario unless otherwise noted. Performance measures are: (a) Pressure at P1 in Vedder Sand, (b) Pressure at P1 in Vedder Sand, assuming half uncertainty in near field and twice uncertainty in far field, (c) Total brine flux across eastern boundary, (d) Same as (c), but with comparison of fault vs. no-fault scenario for Vedder Sand permeabilities, (e) Same as (c), but comparison of near-field Vedder Sand permeability vs. compressibility vs. porosity variation, (f) Pressure at P2 in Vedder Sand.

Figures 3(c) shows sensitivity of flux across the eastern boundary with respect to permeability. This far-field performance measure is strongly affected by the Vedder Sand permeability in the eastern far field. The near-field permeability of the Vedder Sand is important during the first injection decades, while all other permeabilities, including those of the overlying shale, become more relevant during the post-injection phase. (The latter indicates that pressure bleed-off is important for the prediction of far-field performance measures.) Figure 3(d) demonstrates

that sensitivities are affected by the fault property scenario choice in a local sensitivity analysis. The *no-fault scenario* shows increased sensitivity to far-field permeability and reduced sensitivity to near-field permeability compared to the *fault* scenario. This finding is consistent with the pressure results in Figure 2, where the reduced hydraulic interaction across faults cause higher pressure response in the near-field region and reduced pressurization in the far field. As evident in Figure 3(e), the sensitivity of the eastern boundary flux to near-field properties of the Vedder Sand is highest for permeability, followed by compressibility and then by porosity, a finding driven in part by the input parameter variation assumed in the sensitivity study.

Figure 3(f) shows sensitivity to pressure buildup in the Vedder Sand at Point P2, several miles updip of the injection location at the interface between the near-field and far-field regions. The most critical parameter at early injection stages is the sand permeability in the near-field. However, other parameters become more relevant towards the end of injection, the sand permeabilities in the far-field regions as well as the permeabilities of the overlying shale. This suggests that when considering far-field performance measures such as large-scale pressurization or brine migration and evaluating long-term behavior, the near-field properties of the injection formation may be less relevant than the far-field properties of not only the storage reservoir but also of the overlying/underlying shale formations.

4. Summary

We have studied the pressure perturbation and brine migration resulting from a hypothetical CO_2 sequestration project in a faulted sandstone basin in the Southern San Joaquin Valley in California, USA. A systematic local sensitivity study was conducted for two distinctive fault property scenarios to identify key parameters and processes affecting the relevant system behavior. Our study suggests that the resulting dimensionless sensitivity coefficients can reveal important information on the relative significance of uncertain input parameters as is comes to pressure effects near and away from the injection location.

Acknowledgments

The authors wish to thank Christine Doughty of Lawrence Berkeley National Laboratory for a careful review of the manuscript and the suggestion of improvements. Thanks are also due to Jeff Wagoner from Lawrence Livermore National Laboratory for developing the geologic framework model of the Southern San Joaquin Basin. This work was funded by the Assistant Secretary for Fossil Energy, Office of Sequestration, Hydrogen, and Clean Coal Fuels, National Energy Technology Laboratory, of the U.S. Department of Energy.

References

[1] van der Meer, L.G.H., Yavuz, F., 2008. CO_2 storage capacity calculations for the Dutch subsurface, Proceedings GHGT-9, Washington, D.C., 2008.

[2] Nicot, J.P., 2008. Evaluation of large-scale carbon storage on fresh-water section of aquifers: A Texas study. International Journal of Greenhouse Gas Control, 2(4), pp. 582–593.

[3] Birkholzer, J.T., Zhou, Q., Tsang, C.F., 2009. Large-scale impact of CO_2 storage in deep saline aquifers: a sensitivity study on the pressure response in stratified systems. International Journal of Greenhouse Gas Control, 3(2), pp. 181–194.

[4] Yamamoto, H., Zhang, K., Karasaki, K., Marui, A., Uehara, H., Nishikawa, N., 2009. Numerical investigation concerning the impact of CO_2 geologic storage on regional groundwater flow. International Journal of Greenhouse Gas Control, 3(5), pp. 586-599.

[5] Birkholzer, J.T., Zhou, Q., 2009. Basin-scale hydrogeologic impacts of CO_2 storage: capacity and regulatory implications. International Journal of Greenhouse Gas Control, 3(6), pp. 745–756.

[6] Zhou, Q., Birkholzer, J.T., Mehnert, E., Lin, Y.-F., Zhang, K., 2010. Modeling Basin- and Plume-Scale Processes of CO_2 Storage for Full-Scale Deployment. Ground Water, 48(4), pp. 494-514.

[7] Zhou, Q., Birkholzer, J.T., Tsang, C.F., Rutqvist, J., 2008. A method for quick assessment of CO2 storage capacity in closed and semi-closed saline formations. International Journal of Greenhouse Gas Control, 2(4), 626–639.

[8] USGS, 2007. *Petroleum Systems and Geologic Assessment of Oil and Gas in the San Joaquin Basin Province, California.* U.S. Geological Survey, Professional Paper 1713, Edited by Allegra Hosford Scheirer.

[9] Pruess, K. 2005. *ECO2N: A TOUGH2 Fluid Property Module for Mixtures of Water, NaCl, and CO_2*. LBNL-57952, Lawrence Berkeley National Laboratory, Berkeley, CA, USA.

[10] Zhang, K., Wu, Y.S., Pruess, K., 2008. *User's Guide for TOUGH2-MP – A Massively Parallel Version of the TOUGH2 Code*. Report LBNL-315E, Lawrence Berkeley National Laboratory, Berkeley, CA, USA.

[11] Finsterle, S., Multiphase inverse modeling: Review and iTOUGH2 applications. Vadose Zone J., 3: 747–762, 2004.

[12] Finsterle, S., *iTOUGH2 Universal Optimization Using the PEST Protocol*. Report LBNL-LB3698E, Lawrence Berkeley National Laboratory, Berkeley, Calif., July 2010.